

This paper was recommended for publication in revised form by Regional Editor Somanchi V S S N V G Krishna Murthy

## **A CLOSED FORM SOLUTION FOR AC ELECTO-KINETIC-DRIVEN FLOW IN A MICROCHANNEL**

**\*Balaram Kundu**

Department of Mechanical Engineering, Jadavpur  
 University, Kolkata 700032, India

*Keywords: Analytical; Electrical potential; Green's function; Microchannel*

*\* Corresponding author: B. Kundu, Phone: +91-33-2457-2669 (O), +91-33-2416-3508 (R), +91-9874-671897 (M), Fax: +91-2414-6890.*

*E-mail address: bkundu@mech.net.in, bkundu123@rediffmail.com*

### **ABSTRACT**

The electro-osmotic fully-developed flow in a circular micro-channel was studied under an alternative electric field. An analytical approach based on the linearized poisson-Boltzmann equation was selected to obtain an exact solution of the electrical potential inside the channel. The velocity distribution was then determined by using Green's function approach. The velocity distribution has been plotted under a design condition.

### **INTRODUCTION**

The development of lab-on-chip devices involves the incorporation of many of the necessary components and functionality of a typical laboratory on to a small glass or polymer chip. These miniaturized systems are slated to offer significant advantages to analytical chemists as they can, in principle, minimize consumption of reagents (by using smaller sample volumes), lessen analysis times, and reduce operation and manufacturing costs. While species transport on these devices can be accomplished by a number of techniques, for example, pressure or thermo-pneumatically driven flow, the lack of moving parts and the favorable velocity profile have made electro-kinetic means such as electro-osmosis and electrophoresis the preferred method.

The electro-kinetic effects were first discovered by Reuss [1] from an experimental investigation on porous clay, which was followed by experiments of Wiedmann [2]. Helmholtz [3] developed the electric double-layer (EDL) theory relating the electric and flow parameters for electro-kinetic transport. The case of EDL thickness being much smaller than the channel dimensions was analyzed by Von Smoluchowski [4]. He also derived a velocity slip condition

for electro-osmotically driven flows. Electro-osmotic flows in thin two-dimensional slits and thin cylindrical capillaries were analyzed by Burgreen and Nakache [5], and Rice and Whitehead [6], respectively. Overbeek [7] proposed the irrotationality condition of internal electro-osmotic flows for arbitrary shaped geometry. This was followed by the ideal electro-osmosis concept of Cummings et al. [8] who showed similarity between the electric and the velocity fields under some specific outer field boundary conditions.

In the present study, analytical analysis has been conducted to determine the velocity distribution in a circular microchannel under an AC electro-kinetic-driven flow. Using an alternating electrical field, the electro-osmotic fully-developed flow in a circular micro-channel is analyzed. The linearized Poisson-Boltzmann equation has been adopted for the exact solution of the electrical potential inside a channel. The Green's function establishes an exact solution for the velocity distribution.

### **PHYSICAL PROBLEM AND MATHEMATICAL FORMULATIONS**

It is well known that most solid surfaces obtain a surface electric charge when they are brought into contact with a polar medium (e.g. aqueous solutions). This may be due to ionization, ion adsorption or ion dissolution. If the liquid contains a certain amount of ions (for instance, an electrolyte solution or a liquid with impurities), the electrostatic charges on the solid surface will attract the counter-ions in the liquid. The rearrangement of the charges on the solid surface and the balancing charges in the liquid is called the EDL. Immediately next to the solid surface, there is a layer of ions that are

strongly attracted to the solid surface and are immobile. This layer is called the compact layer, normally about several angstroms thick. Because of the electrostatic attraction, the counter-ions concentration near the solid surface is higher than that in the bulk liquid for away from the solid surface. The co-ions concentration near the surface, however, is lower than that in the bulk liquid for away from the solid surface, due to the electrical repulsion. So there is a net charge in the region close to the surface. From the compact layer to the uniform bulk liquid, the net charge density gradually reduces to zero. Ions in this region are affected less by the electrostatic interaction and are mobile. This region is called the diffuse layer of the EDL. The thickness of the diffuse layer is dependent on the bulk ionic concentration and electrical properties of the liquid, usually ranging from several nanometers for high ionic concentration solution up to several microns for pure water and pure organic liquids. The boundary between the contact layer and the diffuse layer is usually referred to as the shear plane. The electrical potential at the solid-liquid surface is difficult to measure directly. The electrical potential at the solid-liquid surface is difficult to measure directly. The electrical potential at the shear plane is called the zeta potential  $\zeta$  and can be measured experimentally. In practice, the zeta potential is used as an approximation to the potential at the solid-liquid interface. For example, a glass surface immersed in water undergoes a chemical reaction in which a fraction of the surface silanol group  $\text{SiOH}$  are changed to  $\text{SiO}^-$  or  $\text{SiOH}_2^+$ , resulting in a net negative or positive surface potential depending on PH of the electrolyte. This influences distribution of the ions in the buffer solution as shown in Fig. 1. The ions of opposite charge cluster immediately near the wall forming the Stern layer, a layer of typical thickness of one ion diameter. The ions within the Stern layer are attracted to the wall with very strong electrostatic forces, as recently shown by molecular dynamics studies. Immediately, after the Stern layer, here forms the electrostatic double layer, where the ion density variation obeys the Boltzmann distribution, consistent with the derivation based on statistical mechanical considerations.

Consider a fully developed flow inside a circular micro-channel that is produced by an electric field in the absence of any pressure gradient. First of all, it is needed to know the local net charge density per unit volume  $\rho_e$  at any point in the solution. This requires solving the EDL field [9–15],

$$\nabla^2 \psi = \frac{2Ze n_0}{\epsilon} \sinh(Ze\psi/k_B T) \quad (1)$$

where,  $\psi$  is the electric potential. For pure electro-osmotic fully developed flow of incompressible fluid in circular microchannels, the Navier-Stokes equations take the following form:

$$\rho \frac{\partial V_z}{\partial t} = \mu \left( \frac{\partial^2 V_z}{\partial r^2} + \frac{1}{r} \frac{\partial V_z}{\partial r} \right) - \rho_e E(\omega t) \quad (2)$$

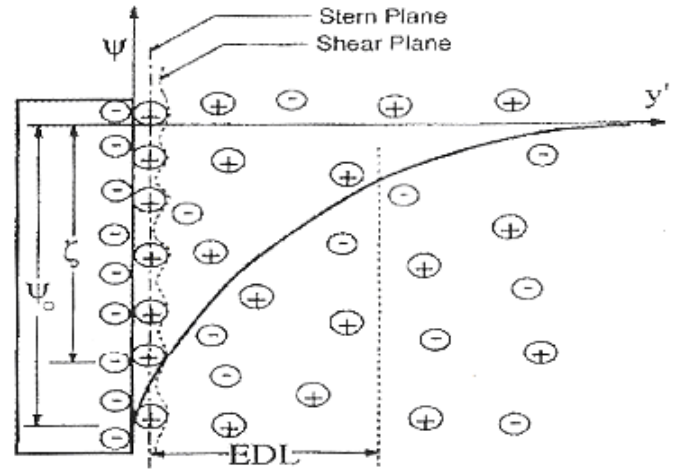


Fig. 1. Schematic diagram of electric double layer (EDL) next to a negatively charged solid surface.

where,  $V_z$  is the only non-zero velocity component along the channel,  $\rho$  and  $\mu$  are the density and viscosity of liquid, respectively, and  $E(\omega t)$  is a general time periodic function with a frequency  $\omega = 2\pi f$  that describes the applied electric field strength.

The boundary conditions for solution of Eqs. (1) and (2) can be written as

$$\text{at } r = 0, \quad \frac{d\psi}{dr} = 0 \quad (3a)$$

$$\text{at } r = \Re, \quad \psi = \zeta \quad (3b)$$

$$\text{at } r = 0, \quad \frac{dV_z}{dr} = 0 \quad (3c)$$

$$\text{at } r = \Re, \quad V_z = 0 \quad (3d)$$

where,  $\Re$  and  $\zeta$  are the channel radius and the zeta potential, respectively. Consider the following dimensionless variables:

$$R = \frac{r}{\Re}; \quad \tilde{\psi} = \frac{Ze}{k_B T} \psi; \quad \theta = \frac{\mu}{\rho \Re^2} t; \quad \Omega = \frac{\rho \Re^2}{\mu} \omega; \quad (4)$$

$$V = \frac{Ze\mu}{\epsilon E_z k_B T} V_z$$

where,  $E_z$  is a constant equivalent to the strength of the applied electric field.

Introducing the above dimensionless variables into Eqs. (1) and (2) gives the following nondimensional forms of the governing equations:

$$\nabla^2 \tilde{\psi} = (\kappa \Re)^2 \sinh(\tilde{\psi}) \quad (5)$$

$$\frac{\partial V}{\partial \theta} = \frac{\partial^2 V}{\partial R^2} + \frac{1}{R} \frac{\partial V}{\partial R} + (\kappa \mathfrak{R})^2 \sinh(\tilde{\psi}) F(\Omega \theta) \quad (6)$$

where,  $F(\Omega \theta)$  is a general periodic function of unit magnitude such that  $E(\Omega \theta) = E_z F(\Omega \theta) \kappa$  is the Debye-Huckel parameter defined as follows:

$$\kappa = \left( \frac{2Z^2 e^2 n_\infty}{\epsilon \epsilon_0 k_B T} \right)^{1/2} \quad (7)$$

The boundary conditions (Eq. 3) can be written in dimensionless form as

$$\text{at } R=0, \quad \frac{d\tilde{\psi}}{dR} = 0 \quad (8a)$$

$$\text{at } R=1, \quad \tilde{\psi} = Z \quad (8b)$$

$$\text{at } R=0, \quad \frac{dV}{dR} = 0 \quad (8c)$$

$$\text{at } R=1, \quad V = 0 \quad (8d)$$

In Eq. (5) under a condition, the double layer potential  $\tilde{\psi}$  is small and therefore it can be linearized by the so called Debye-Huckel approximation as

$$\frac{d^2 \tilde{\psi}}{dR^2} + \frac{1}{R} \frac{d\tilde{\psi}}{dR} = K^2 \tilde{\psi} \quad (9)$$

where,  $K = \kappa \mathfrak{R}$  and it is called electro-kinetic radius.

Equation (11) is solved by using Eq. (8) as [16–21]

$$\tilde{\psi}(R) = \frac{Z}{I_0(K)} I_0(KR) \quad (10)$$

where,  $I_0(K)$  is the modified Bessel function of first kind order zero and argument  $K$ . In order to solve Eq. (6), the

Debye-Huckel approximation is implemented to result in the following form of the equation:

$$\frac{\partial V}{\partial \theta} = \frac{\partial^2 V}{\partial R^2} + \frac{1}{R} \frac{\partial V}{\partial R} + K^2 \tilde{\psi}(R) F(\Omega \theta) \quad (11)$$

The Green's function approach is now used to find an analytical solution for the non-dimensional form of Eq. (11),

$$\frac{\partial G}{\partial \theta} - \frac{1}{R} \frac{\partial}{\partial R} \left( R \frac{\partial G}{\partial R} \right) = \frac{\delta(R-l) \delta(\theta-\tau)}{2\pi R} \quad (12)$$

$$\begin{cases} \lim_{R \rightarrow 0} |G(R, \theta; l, \tau)| < \infty \\ G(1, \theta; l, \tau) = 0 \end{cases} \quad 0 < R, l < 1, 0 < \theta, \tau \quad (13)$$

where,  $\delta(x)$  is Dirac delta function. We can start with considering Laplace transform on Eq. (12) as

$$\frac{1}{R} \frac{\partial}{\partial R} \left( R \frac{\partial G}{\partial R} \right) - sG = \frac{-e^{-s\tau}}{2\pi R} \delta(R-l) \quad (14)$$

Next  $\delta(R-l)/R$  is expressed as a Fourier-Bessel expansion as

$$\frac{\delta(R-l)}{2\pi R} = \sum_{n=1}^{\infty} A_n J_0(\lambda_n l) \quad (15)$$

where,  $\lambda_n$  is the n-th root of the solution of  $J_0(\lambda) = 0$ .  $A_n$  can be determined from the following equation:

$$A_n = \frac{2}{J_1^2(\lambda_n)} \int_{R=0}^1 \frac{\delta(R-l)}{2\pi R} J_0(\lambda_n R) R dR = \frac{J_0(\lambda_n l)}{\pi J_1^2(\lambda_n)} \quad (16)$$

Combining Eqs. (14), (15), and (16) yields,

$$\frac{1}{R} \frac{\partial}{\partial R} \left( R \frac{\partial G}{\partial R} \right) - sG = \frac{-e^{-s\tau}}{\pi} \sum_{n=1}^{\infty} \frac{J_0(\lambda_n l) J_0(\lambda_n R)}{J_1^2(\lambda_n)} \quad (17)$$

The solution to Eq. (17) is

$$G(R, \theta; l, \tau) = \frac{H(\theta-\tau)}{\pi} \sum_{n=1}^{\infty} \frac{J_0(\lambda_n l) J_0(\lambda_n R)}{J_1^2(\lambda_n)} e^{-\lambda_n^2(\theta-\tau)} \quad (18)$$

where,  $H(x)$  is the Heaviside step function. Now the velocity is determined by using boundary conditions (8c) and (8d)

$$V(R, \theta) = \int_0^l \int_0^1 G(R, \theta; l, \tau) Q(l, \tau) dl d\tau \quad (19)$$

If the periodic function is  $F(\Omega \theta) = \sin(\Omega \theta)$ , taking the above integrals will give the non-dimensional velocity profile:

$$V(R, \theta) = \frac{K^2 Z}{\pi I_0(K)} \sum_{n=1}^{\infty} \frac{J_0(\lambda_n l) \left[ \lambda_n^2 \sin(\Omega \theta) - \cos(\Omega \theta) + \Omega e^{-\lambda_n^2 \theta} \right]}{(\lambda_n^4 + \Omega^2) J_1^2(\lambda_n)} \quad (20)$$

where

$$U = \int_0^l J_0(\lambda_n l) I_0(Kl) dl \quad (21)$$

Equation (21) can be expanded as

$$U = 1 + \frac{1}{12} (K^2 - \lambda_n^2) + \frac{1}{30} (K^4 + \lambda_n^4) - \frac{1}{16128} (K^6 - \lambda_n^6) + \frac{1}{1327104} (K^8 + \lambda_n^8) - \frac{1}{80} \lambda_n^2 K^2 + \frac{\lambda_n^2 K^2}{1792} (\lambda_n^2 - K^2)$$

$$\begin{aligned}
 & -\frac{\lambda_n^2 K^2}{82944}(\lambda_n^4 + K^4) + \frac{1}{36864} \lambda_n^4 K^4 \\
 & + \frac{\lambda_n^4 K^4}{1622016}(K^2 - \lambda_n^2) + \frac{\lambda_n^2 K^2}{6488064}(\lambda_n^6 - K^6) + \dots
 \end{aligned} \quad (22)$$

## RESULTS AND DISCUSSIONS

In the present analytical description of electro-osmotic flow in a circular micro-channel, the governing parameter is  $\Omega$  which represents the ratio of the diffusion time scale ( $t_{diff} = \rho R^2 / \mu$ ) to the period of the applied electric field ( $tE = 1/\omega$ ). Figs. 2 shows the time periodic velocity profiles in a circular channel for  $\Omega = 30$ . This  $\Omega$  value correspond to frequencies of 500 Hz in a 100  $\mu\text{m}$  channel. To illustrate the essential features of the velocity profile, a relatively large double layer thickness has been used,  $\kappa = 6 \times 10^6 \text{ m}^{-1}$  (corresponding to bulk ionic concentration  $n_\infty = 10^{-6} \text{ M}$ ), and a uniform surface potential  $\zeta = 12.5 \text{ mV}$  was used (within the bounds imposed by the Debye–Huckel linearization). From Fig. 2, it is apparent that the application of the electric body force results in a rapid acceleration of the fluid within the double layer and fluid motion is observed throughout the fluid. Figure 2 shows the nondimensional velocity profiles using sinusoidal wave at  $\Omega\theta = \omega t = \pi/2, \pi, 3\pi/2$ , and  $2\pi$ . As expected, when  $\Omega$  is increased, the phase shift for both the double layer and bulk flow velocities are increased because of the number of cycles required to reach the steady state. It is interesting to note the net positive or negative velocity at the channel midpoint within the transient period before decaying into the steady state behavior. This is a result of the initial positive or negative impulse given to the system when the electric field is first applied. The transient oscillations are observed to decay at an exponential rate, as expected from the transient term. Similar to the out-of-phase cosine term, this exponential term is also proportionally scaled by the non-dimensional frequency, suggesting that the effect of the initial impulse becomes more significant with increasing  $\Omega$ .

## CONCLUSIONS

In the present study, an analytical analysis based on the linearized Poisson–Boltzmann equation has been developed for liquid flow in a circular micro-channel induced by unsteady applied electric fields. In this analytical description of electro-osmotic flow in a circular micro-channel, the governing parameter is  $\Omega$  which represents the ratio of the diffusion time scale ( $t_{diff} = \rho R^2 / \mu$ ) to the period of the applied electric field ( $t_E = 1/\omega$ ). At every case study for varying  $\omega t$ , steady state has been achieved with a high value of  $R$ .

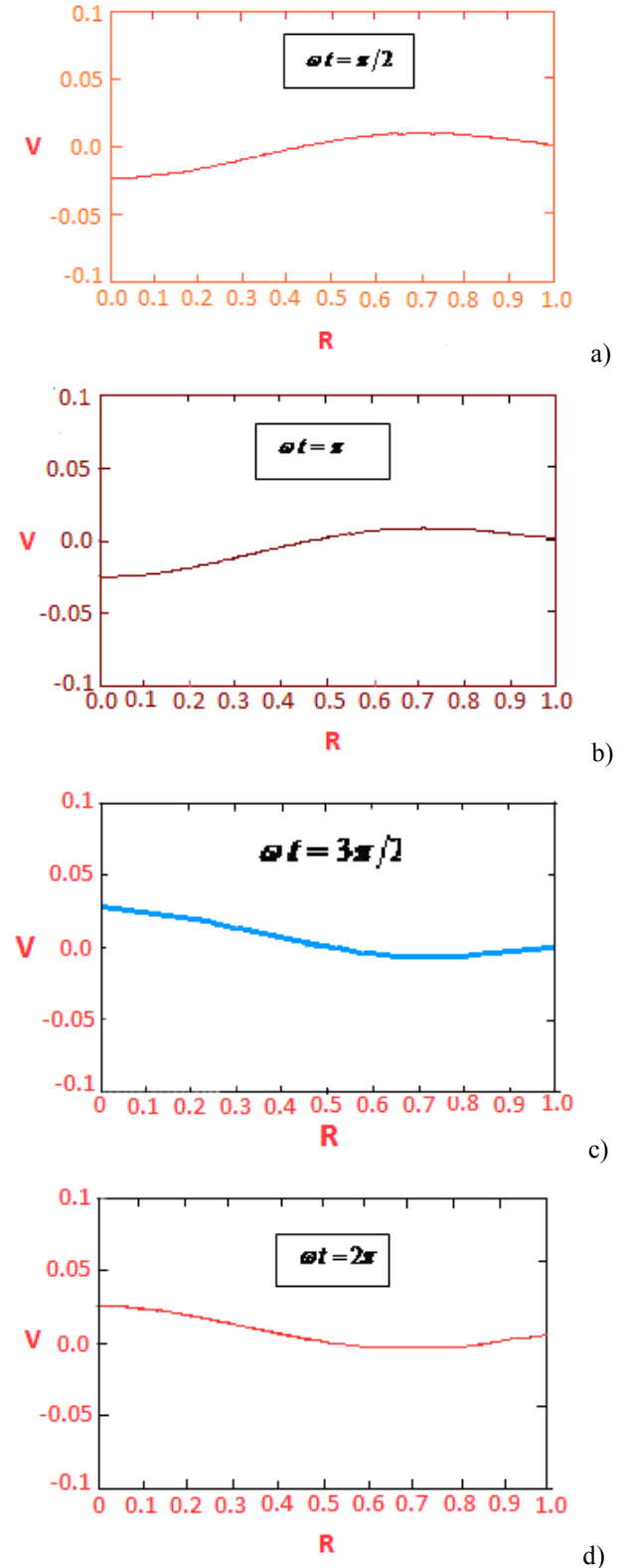


Fig. 2. Steady state time periodic non-dimensional velocity profiles with  $\kappa R = 300$  for one period ( $0 \leq \Omega\theta \leq 2\pi$ ) of the sinusoidal waveform at  $\Omega = 30$ : (a)  $\omega t = \pi/2$ , (b)  $\omega t = \pi$ , (c)  $\omega t = 3\pi/2$ , (d)  $\omega t = 2\pi$ .

**NOMENCLATURE**

$e$	Absolute charge of electron
$E(\omega t)$	general time periodic function, see Eq. (2)
$E_z$	strength of the applied electric field, see Eq. (4)
EDL	electric double layer
$f$	frequency
$I_n(x)$	modified Bessel function of first kind of order $n$ and argument $x$
$J_n(x)$	Bessel function of first kind of order $n$ and argument $x$
$k$	Debye-Huckel parameter
$K$	Electro-kinetic radius, $k \mathfrak{R}$
$K_B$	Boltzmann constant
$n_0$	ion density
$n_\infty$	number of electrons
$r$	radial coordinate
$R$	dimensionless radial coordinate, $r/\mathfrak{R}$
$\mathfrak{R}$	Channel radius
$t$	time
$T$	temperature
$v$	velocity component along the channel
$V$	dimensionless velocity defined in Eq. (4)
$V_z$	Helmholtz–Smoluchowski electro-osmotic velocity
$y'$	distance measured from the wall
$Z$	Valence
<i>Greek Letters</i>	
$\delta(x)$	direct delta function
$\varepsilon$	permittivity
$\varepsilon_0$	
$\mu$	viscosity
$\zeta$	electric potential at the shear plane (zeta potential)
$\Omega$	dimensionless parameter defined in Eq. (4)
$\psi$	electric potential
$\tilde{\psi}$	dimensionless electric potential, $Ze\psi/K_B T$
$\psi_0$	surface electric potential
$\theta$	dimensionless time, $t\mu/\mathfrak{R}^2\rho$
$\omega$	angular speed
$\rho$	density
$\rho_e$	local charge density per unit volume

**REFERENCES**

[1] F. Reuss, Sur un nouvel effet de l'electricite galvanique. Memoires de la Societe Imperiale de Naturalistes de Moscou, 2 (1809) 327-337.

[2] Wiedemann, G. *Pogg. Ann.* 1852, 87, 321.  
 [3] H. Helmholtz, Uber den einfluß der elektrischen grenzschichten bei galvanischer spannung und der durch wasserstromung erzeugten potentialdifferenz, *Ann.* 7 (1879) 337.  
 [4] M. von Smoluchowski, Versuch einer mathematischen theorie der kogulationskinetic kolloid losunaen, *Z. Phys. Chem.* 92 (1917) 129–35.  
 [5] D. Burgreen and F.R. Nakache, Electrokinetic flow in ultrafine capillary slits. *J. Phys. Chem.* 68 (1964) 1084–1091.  
 [6] C.L. Rice and R. Whitehead, Electrokinetic flow in a narrow cylindrical capillary. *J. Phys. Chem.* 69 (1964) 4017–4024.  
 [7] J.T.G. Overbeek, Phenomenology of lyophobic systems. In: Kruyt HR (ed) Colloid science, vol 1. Elsevier, Amsterdam, pp 58–59, 1952.  
 [8] E.B. Cummings, S.K. Griffiths, R.H. Nilson, Irrotationality of uniform electro-osmosis, *Proc SPIE Microfluidic Devices Syst II*:180–189, 1999.  
 [9] S. Kandlikar, S. Garimella, D. Li, S. Colin, M.R. King, *Heat Transfer and Fluid Flow in Minichannels and Microchannels*, Elsevier, 2006.  
 [10] A. Ajdari, Electroosmosis on inhomogeneously charged surfaces, *Phys. Rev. Lett.* 75 (1995) 755–758.  
 [11] D. Erickson, D. Li, Analysis of AC electroosmotic flows in a rectangular microchannel, *Langmuir* 19 (2003) 5421–543.  
 [12] A. Gonzalez, A. Ramos, N.G. Green, A. Castellanos, H. Morgan, Fluid flow induced by non-uniform AC electric fields in electrolytes on microelectrodes II: a linear double layer analysis, *Phys. Rev. E* 61 (2000) 4019–4028.  
 [13] A.B.D. Brown, C.G. Smith, A.R. Rennie, Pumping of water with an AC electric field applied to asymmetric pairs of microelectrodes, *Phys. Rev. E* 63 (2002) 016305 1–8.  
 [14] P. Tabeling, *Introduction to Microfluidics*, Oxford University Press, 2005.  
 [15] R. Haberman, *Elementary Applied Partial Differential Equations*, Prentice Hall, 987.  
 [16] B. Kundu, K.-S. Lee, Thermal design of an orthotropic flat fin in fin-and-tube heat exchanger operating in dry and wet environments, *International Journal of Heat and Mass Transfer* 54 (2011), Nos. 25-26, 5207–5215.  
 [17] B. Kundu, Performance and optimization of flat plate fins of different geometry on a round tube: A comparative investigation, *Journal of Heat Transfer–Transactions of ASME* 129 (7) (2007) 917–926.  
 [18] B. Kundu, P.K. Das, Performance analysis and optimization of elliptic fins circumscribing a circular tube, *International Journal of Heat and Mass Transfer* 50 (1-2) (2007) 173–180.  
 [19] B. Kundu, P.K. Das, Performance analysis of eccentric annular fins with a variable base temperature, *Numerical Heat Transfer Part A-applications* 36 (7) (1999) 751–766.  
 [20] B. Kundu, P.K. Das, Performance analysis and optimization of eccentric annular disc fins, *Journal of*

Heat Transfer–Transactions of ASME 105 (1) (1999)  
128–135.

- [21] B. Kundu, P.K. Das, Optimum dimensions of plate fins for fin tube heat exchangers, International Journal of Heat and Fluid Flow 18 (5) (1997) 530